The TORC1/TORC2 inhibitor, Palomid 529, reduces tumor growth and sensitizes to docetaxel and cisplatin in aggressive and hormone-refractory prostate cancer cells

Giovanni Luca Gravina[1,2], Francesco Marampon[1,2], Foteini Petini[1], Leda Biordi[3], David Sherris[5], Emmanuele A Jannini[4], Vincenzo Tombolini[2] and Claudio Festuccia[1]

[1]Laboratory of Radiobiology, [2]Division of Radiotherapy, [3]Oncology and [4]Endocrinology, Department of Experimental Medicine, University of L'Aquila, Via Vetoio, Coppito 2, 67100 L'Aquila, Italy
[5]Paloma Pharmaceuticals, Inc., Jamaica Plain, Massachusetts, USA

(Correspondence should be addressed to C Festuccia; Email: claudio.festuccia@univaq.it)

Abstract

One of the major obstacles in the treatment of hormone-refractory prostate cancer (HRPC) is the development of chemo-resistant tumors. The aim of this study is to evaluate the role of Palomid 529 (P529), a novel TORC1/TORC2 inhibitor, in association with docetaxel (DTX) and cisplatin (CP). This work utilizes a wide panel of prostatic cancer cell lines with or without basal activation of Akt as well as two *in vivo* models of aggressive HRPC. The blockade of Akt/mTOR activity was associated to reduced cell proliferation and induction of apoptosis. Comparison of IC50 values calculated for PTEN-positive and PTEN-negative cell lines as well as the PTEN transfection in PC3 cells or PTEN silencing in DU145 cells revealed that absence of PTEN was indicative for a better activity of the drug. In addition, P529 synergized with DTX and CP. The strongest synergism was achieved when prostate cancer (PCa) cells were sequentially exposed to CP or DTX followed by treatment with P529. Treatment with P529 before the exposure to chemotherapeutic drugs resulted in a moderate synergism, whereas intermediated values of combination index were found when drugs were administered simultaneously. *In vivo* treatment of a combination of P529 with DTX or CP increased the percentage of complete responses and reduced the number of mice with tumor progression. Our results provide a rationale for combinatorial treatment using conventional chemotherapy and a Akt/mTOR inhibitor as promising therapeutic approach for the treatment of HRPC, a disease largely resistant to conventional therapies.

Endocrine-Related Cancer (2011) **18** 385–400

Introduction

Prostate cancer (PCa) represents a global public health problem. Worldwide, it is the second most common non-cutaneous cancer in men, accounting for 10% of male cancers. In recent years, 5-year survival rates for PCa have been ranked third highest of all cancers (Desireddi *et al*. 2007, Svatek *et al*. 2008). Although chemotherapy historically has had limited utility in treating advanced PCa, the results from two recent randomized clinical trials indicated that docetaxel (DTX)-based chemotherapy improved survival in patients with hormone-refractory prostate cancer (HRPC; Patel *et al*. 2005, Armstrong *et al*. 2007). Some clinical studies supported taxane-based therapy as a promising platform to develop a new combinational schedule, which remains a high priority for many ongoing studies (Patel *et al*. 2005, Armstrong *et al*. 2007, Calabrò & Sternberg 2007). In addition, a recent report shows that single-agent satraplatin improves progression-free survival (PFS) as second-line chemotherapy for patients with HRPC and provides further evidence that platinum salts may have a role in the

DOI: 10.1530/ERC-11-0045
1351–0088/11/018–385
Online version via http://www.endocrinology-journals.org

treatment of this disease (Nakabayashi *et al*. 2008, Ross *et al*. 2008). Nevertheless, improvement in the efficacy of chemotherapy is urgently needed for patients with chemo-resistant HRPC.

It is imperative not only to discover the molecular basis of resistance but also to find therapeutic agents that can disrupt the resistant pathways. An important role in drug and anti-hormone resistance is played by the phosphatidylinositol-3-kinase (PI3K)/Akt (protein kinase B (PKB)) signaling pathway. PI3K is a heterodimeric enzyme composed of a 110 kDa catalytic subunit and an 85 kDa regulatory subunit. PI3K catalyzes the production of PtdIns-3,4-P2 and PtdIns-3,4,5-P3 helping to recruit Akt (PKB) and PDK1 to the membrane. When activated, Akt transmits survival signals from growth factors and inactivates the apoptotic pathways. PTEN (phosphatase and tensin homolog deleted on chromosome 10)/mutated in multiple advanced cancers (MMAC) is a tumor suppressor gene. PTEN is lost or mutated in a large number of human cancers including PCa (Wu *et al*. 1998, Trotman *et al*. 2003, Wang *et al* 2003, Ma *et al*. 2005, Bertram *et al*. 2006, Verhagen *et al*. 2006). Deregulation of PI3K pathway is commonly observed in many human cancers. This deregulation can be caused either by loss of PTEN, or by constitutive activation of PI3K or its target Akt. Activation of PI3K/Akt may potentiate cell survival, cell migration, proliferation, and cytoskeletal rearrangement. In addition, PI3K pathway is implicated in upregulating vascular endothelial growth factor (VEGF; Shukla *et al*. 2005). It has also been demonstrated that Akt activity correlates with PCa progression and poor clinical outcome (Graff *et al*. 2000, Murillo *et al*. 2001, Uzgare & Isaacs 2004, Xu *et al*. 2006, Banach-Petrosky *et al*. 2007, Bedolla *et al*. 2007, Festuccia *et al*. 2007, El Sheikh *et al*. 2008, Festuccia *et al*. 2008). Increasing evidence supports the concept that Akt inhibition can be crucial for Pca therapy.

The novel compound 8-(1-hydroxy-ethyl)-2-methoxy-3-(4-methoxy-benzyloxy)-benzo[*c*]chromen-6-one (Palomid 529 (P529)) has been recently shown to target Akt/mTOR pathways, exhibiting selective anti-proliferative activity for endothelial cells (Xue *et al*. 2008, Xiang *et al*. 2011) and sensitizing Pca cells to radiotherapy (Diaz *et al*. 2009). P529 is also able to dissociate the TORC1 and TORC2 complexes, resulting in the inhibition of mTOR activity. The mTOR protein is a cytosolic serine/threonine kinase serendipitously discovered in the 1990s when the mechanism of action of rapamycin was investigated. mTOR complexes with raptor (regulatory associated protein of mTOR) and rictor (rapamycin insensitive companion of mTOR) to form mTOR complex 1 (mTORC1) and mTORC2, respectively. mTORC1 is downstream to Akt and is susceptible to inhibition by rapamycin and its analogs, whereas mTORC2 is an upstream regulator of Akt, and the activity is upregulated in certain circumstances as a compensatory response to mTORC1 inhibition.

This work utilizes a wide panel of prostatic cancer cell lines with or without basal activation of Akt and two *in vivo* models of aggressive HRPC. HRPC is a disease with very complex and heterogeneous molecular traits. No commonly used cell line represents all aspects of HRPC. PC3 and DU145 cell lines have been extensively used in the past to study HRPC. These cells are insensitive to androgens, lacking androgen receptors (ARs). However, the majority of human HRPC have high levels of AR and the AR pathways are active even in the absence of androgens. It has been also demonstrated that the levels of AR are upmodulated from Akt (Ha *et al*. 2011). Therefore, PCa cell lines can be useful to circumvent individual molecular rearrangements, typical of each cell line, and in most cases representative of the genetic diversity of human PCa. Here, we show that inhibition of the Akt pathway blocks the cell cycle progression in the G0/G1 phase of PCa cells and induces apoptosis in a time- and dose-dependent manner, and enhances the sensitivity to DTX and cisplatin both *in vitro* and *in vivo*. We conclude that the Akt pathway might play an important role in inducing resistance to chemotherapeutic drugs in PCa cells and targeting the Akt pathway might be a promising strategy for enhancing sensitivity to DTX and cisplatin mainly in HRPC.

Materials and methods

Reagents

All the materials for tissue culture were purchased from Hyclone (Cramlington, NE, USA). Plasticware was obtained from Nunc (Roskilde, Denmark). Antibodies were purchased from Santa Cruz (Santa Cruz, CA, USA) unless otherwise indicated. Akt/PKB kinase activity was performed using a non-radioactive assay kit, which was purchased from Stressgene Bioreagents (Victoria, BC, Canada). The antibody recognizing the 46 kDa (pro-form) and 35 kDa (cleaved form) of caspase-9 was purchased from Epitomics (Burlingame, CA, USA). SiRNA for PTEN was purchased from Santa Cruz. Caspase-3 activity was assessed using a commercially available kit (Trevigen, Gaithersburg, MD, USA).

Cell lines

Two non-tumor prostate epithelial cell lines (BPH1 and EPN (Sinisi *et al*. 2002)), 19 PCa cells lines (CWR22 (Tepper *et al*. 2002), CWR22R-2152 (Tepper *et al*. 2002), CWR22R-2272 (Tepper *et al*. 2002), CWR22R-2274 (Tepper *et al*. 2002), CWR22R-2524 (Tepper *et al*. 2002), 22rv1 (Sramkoski *et al*. 1999), LAPC-4 (Craft *et al*. 1999), LnCaP, LnCaP-C81 (Igawa *et al*. 2002), LnCaP-104S (Kokontis *et al*. 1998), LnCaP-104R1 (Kokontis *et al*. 1998), C4-2B (Lin *et al*. 2001), DU145, PC3, VCaP (Chay *et al*. 2002) and DuCaP (Chay *et al*. 2002), PTEN-transfected PC3 (Zhao *et al*. 2004) and AR-transfected PC3 (Bonaccorsi *et al*. 2000), and DU145 (Scaccianoce *et al*. 2003) cells were used (a complete characterization of these cell models is reviewed in Pienta *et al*. (2008)).

Growth assays

Cells were seeded at a density of 2×10^4 cells/ml in 24-well plates. They were left to attach and grow in a 5% FCS DMEM for 24 h. The cells were then maintained in appropriate culture conditions. Morphological controls were performed every day with an inverted phase-contrast photomicroscope (Nikon Diaphot, Tokyo, Japan), before cell trypsinization and counting. Cells trypsinized and resuspended in 1.0 ml of saline were counted using the NucleoCounter NC-100 (automated cell counter systems, Chemo-Metec, A/S, Allerød, Denmark). All experiments were conducted in triplicate. IC_{50} values were calculated by the GraFit method (Erithacus Software Limited, Staines, UK), considering the slopes of inhibition curves obtained for each group of tests. The effect on cell proliferation was measured by calculating the mean cell number with respect to controls in the time for the different treatment groups.

Drugs and preparation

P529 (Paloma Pharmaceuticals, Jamaica Plain, MA, USA) was stored as a dimethylsulfoxide (DMSO)-dissolved powder at 4 °C and suspended in medium on the day of use. A stock solution of P529 was prepared as an aqueous micronized (particle size $<1\,\mu$) formulation. This formulation is a semi-stable suspension of 14 mg/ml P529 requiring gentle vortexing to retain suspension. The micronized formulation contains 0.2% tyloxapol (non-ionic detergent) in Alcon balanced salt buffer. DTX and cisplatin (Sanofi–Aventis Pharmaceuticals, Inc., Bridgewater, NJ, USA) were obtained from the hospital pharmacy.

In vitro drug combination studies

The MTT cytotoxicity assay was used to examine cell survival after combinations of P529 and CP and DTX. Drug combination studies were based on concentration effect curves generated as a plot of the fraction of unaffected (surviving) cells versus drug concentration (Chou & Talalay 1984). Serial dilutions of equipotent doses of the two agents in combination were tested. Synergism, additivity and antagonism were quantified by determining the combination index (CI) calculated by the Chou–Talalay equation, as described elsewhere (Bruzzese *et al*. 2006, Di Gennaro *et al*. 2010). Using the computer program CalcuSyn (Biosoft, Cambridge, UK), the CI for every combination was computed. A CI <0.9, CI $=0.9$–1.2 and CI >1.2 indicated synergistic, additive, and antagonistic effect, respectively. Dose reduction index (DRI) represents the measure of how much the dose of each drug in a synergistic combination may be reduced at a given effect level compared with the doses of each drug alone (Chou & Talalay 1984).

Preparation of cell lysates and western blot analysis

Following treatments, cells, grown in 90 mm diameter petri dishes, were washed with cold PBS and immediately lysed with 1 ml lysis buffer containing a proteinase and phosphatase inhibitor cocktail. Lysates were electrophoresed in a 7% SDS-PAGE, and separated proteins were transferred to nitrocellulose and probed with appropriate antibodies using the conditions recommended by the suppliers.

Cell cycle and apoptosis analysis

Adherent cells were trypsinized, pooled with the culture supernatant containing the apoptotic cells already detached from the dish and centrifuged. Cells (1×10^6) were washed in PBS and fixed for 30 min by the addition of 1 ml of 70% ethanol. After 30 min, the cells were pelleted by centrifugation (720 ***g***; 5 min), and resuspended in 1 ml DNA staining solution (PBS containing 200 mg/ml RNase A, 20 mg/ml propidium iodide plus 0.1% Triton X-100) and stained by incubation at room temperature for 60 min. Apoptosis were analyzed also by using the annexin V staining (GenScript, Piscataway, NJ, USA). All cells were then measured on a FACScan flow cytometer (FACScan; Becton Dickinson, Mountain View, CA, USA) with an Argon laser at 488 nm for excitation and analyzed using Cell Quest Software (Becton Dickinson). Apoptotic cells were detected both by the quantifiable

peak in sub-G1 phase, corresponding to the red fluorescence light emitted by sub-diploid nuclei of cells, and by the percentage of annexin V-stained cells. Results were expressed as the percentage of death by apoptosis induced by a particular treatment.

In vivo experiments and evaluation of treatment response

Male CD1 nude mice (Charles River, Milan, Italy) were maintained under established guidelines (University of L'Aquila, Medical School and Science and Technology School Board Regulations, complying with the Italian government regulation no. 116, January 27 1992 for the use of laboratory animals). All mice received s.c. flank injections of 1×10^6 PC3 and 22rv1 cells. Treatments were initiated when tumor volumes were about 80 mm^3. Tumor growth was assessed by biweekly measurement of tumor diameters with a Vernier caliper (length $\times$ width). Tumor volume was calculated according to the formula: TV (mm^3) $=\pi\times d^2\times D/2$, where d and D are the shortest and longest diameters, respectively (Prewett *et al*. 2002).

Protocol 1

Four groups of 10 mice each were used to determine the *in vivo* effect of different doses of P529 (50, 100, and 200 mg/kg) administered by oral gavage (5 days/week for 4 or 5 weeks). Control mice received same amount of vehicle alone.

Protocol 2

Six groups of 12 mice each were used to determine the effect of P529 (100 mg/kg) administered by oral gavage (5 days/week for 4 or 5 weeks) in combination with DTX (i.p. injection of 7.5 mg/kg per week) or cisplatin (30 mg/kg q21day).

The treatments were stopped when tumors in the control group reached the average volume of about 2500 mm^3 (maximal ethically acceptable volume). The effects of the treatments were examined as described previously (Prewett *et al*. 2002).

Tumor growth delay (TGD) was determined as %TGD$=((T_C)/C)_100$, where T and C are the mean times in days required to reach the same fixed tumor volume in the treated group and control group, respectively (Bruzzese *et al*. 2006). *In vivo* drug combination studies were evaluated by CalcuSyn (Biosoft). For the calculation of CI, the values of cell kill for a fixed tumor volume were considered (determined by the log cell kill (LCK)). LCK was determined as $LCK=(T-C)/(3.3-T_d)$, where T_d represents the mean control group doubling time required to reach a fixed tumor volume, expressed in days, whereas T and C are the same values as described above (Bruzzese *et al*. 2006).

Manipulation of tumor tissue samples

Animals were killed by carbon dioxide treatment and the tumors were subsequently removed surgically. Half of the tumor was directly frozen in liquid nitrogen for protein analysis and the other half fixed in paraformaldehyde overnight for immunohistochemical analyses. Tumor sections were also processed and subjected to standard staining with a Masson trichromic staining kit (HD Supplies, Aylesbury, Buckinghamshire, UK). To identify infiltrating blood vessels (angiogenesis) and to evaluate the expression of proliferation marker (KI67), p-Akt, VEGF and tunnel (apoptosis), immunohistochemistry was carried out on 5 μm de-paraffinized sections using a specific blood vessel staining kit (CD31 or von Willebrand), Ki67, and by apoptotis staining kit (Trevigen). Negative controls were incubated only with universal negative control antibodies under identical conditions, processed, and mounted. Images of the stained blood vessels were taken using a Leitz photo microscope. Positive tumor microvessels were counted at $\times400$ in five arbitrarily selected fields/tumor and the data are presented as number of $CD31^+$ microvessels/$\times100$ microscopic field for each group.

Statistical analysis

Continuous variables were summarized as mean and S.D. or as median and 95% CI for the median. For continuous variables not normally distributed, statistical comparisons between control and treated groups were established by carrying out the Kruskal–Wallis tests. When Kruskal–Wallis tests revealed a statistical difference, pairwise comparisons were made by Dwass–Steel–Chritchlow–Fligner method and the probability of each presumed 'non-difference' was indicated. For continuous variables normally distributed, statistical comparisons between control and treated groups were established by carrying out the ANOVA test or by Student's t test for unpaired data (for two comparisons). When ANOVA test revealed a statistical difference, pairwise comparisons were made by Tukey's honestly significant difference (HSD) test and the probability of each presumed 'non-difference' was indicated. Dichotomous variables were summarized by absolute and/or relative frequencies. For dichotomous variables, statistical comparisons between control and treated groups were established by carrying out the exact Fisher's test. For multiple

comparisons, the level of significance was corrected by multiplying the *P* value by the number of comparisons performed (*n*) according to Bonferroni correction. Time to progression (TTP) was analyzed by Kaplan–Meier curves and Gehan's generalized Wilcoxon test. When more than two survival curves were compared, the Logrank test for trend was used. This tests the probability that there is a trend in survival scores across the groups. All tests were two-sided and were determined by Monte Carlo significance. *P* values <0.05 were considered statistically significant. SPSS (statistical analysis software package, IBM Corp., Armonk, NY, USA) version 10.0 and StatDirect (version. 2.3.3., StatDirect Ltd, Altrincham, Manchester, UK) were used for statistical analysis and graphic presentation.

Results

In vitro experiments

Effect of P529 as single agent. Concentration-dependent and time-dependent effects of P529 on intracellular signaling and proliferation in PCa cell lines

Cells exposed to increasing concentrations of P529 *in vitro* for different times were lysed and analyzed. P529 resulted in a dose- and time-dependent decrease in Akt activity in PC3, LnCaP, and 22rv1 cells as evidenced by a reduced phosphorylation of Akt (Ser^{473}). In Fig. 1, we show the western blotting analyses performed in the PC3 cell line used as the representative model. Similar results were observed in all PCa cells with similar enzymatic IC_{50} values of about 0.2 μM. In the panel 1A, a time-dependent

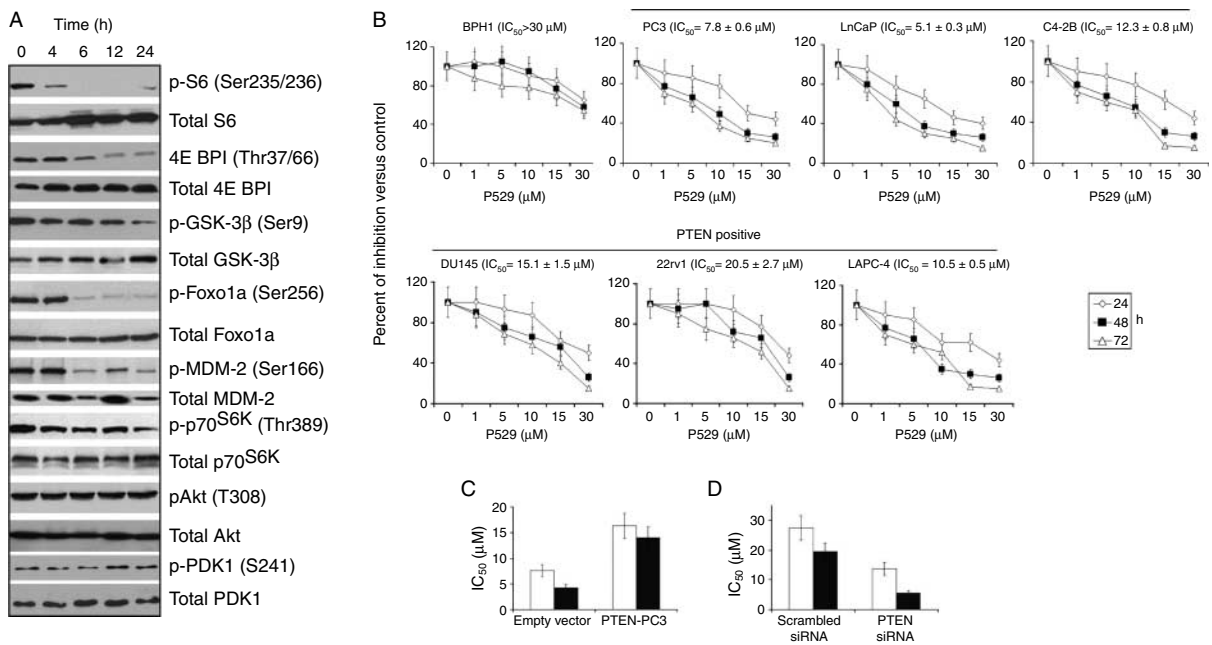

Figure 1 (A) Biochemical evaluation of *in vitro* effects of P529. Prostate cancer cell lines were cultured for 24 h in the presence of different doses of P529 and for different times in presence of 1.0 μM P529 in medium containing 0.5% FBS. Akt activity and phosphorylation were analyzed. Time-dependent experiments showing the western blotting analyses performed in PC3 cells treated with 1.0 μM P529. Total cell extracts were blotted to analyze the levels of dephosphorylated forms of PI3K/TORC1/2 effectors, including $S6^{Ser235/236}$, 4E-$BP^{Thr37/66}$, GSK3β ^{Ser9}, Fox01a^{Ser256}, $MDM2^{Ser166}$, and p70S6k^{Thr389}. Each western blot lane was loaded with 40 μg proteins and normalized versus actin. These experiments are representative of three individual experiments. (B) Anti-proliferative effects of P529. Dose-dependent experiments were performed at 24, 48, and 72 h in a non-cancer cell line (BPH1) and three neoplastic PTEN-negative (PC3, C4-2B and LnCaP) and PTEN-positive (DU145, LAPC-4, and 22rv1) PCa cell lines. Data presented in the graphs pictured in the panel D have been evaluated for statistical analysis by using ANOVA test for linear trend. P529 significantly reduced ($P<0.001$) the Akt activity in all PCa cell lines tested for this analysis. The assessment of IC_{50} values has been performed using Grafit method. (C and D) Role of PTEN. PTEN stable tranfection performed in PC3 cells reduces IC_{50} value for P529 (and thus increases the P529 effectiveness) compared with cells tranfected with empty vector. White columns represent data obtained from the analyses assessed at 24 h of treatment, whereas black columns represent data assessed after 48 h of treatment. We performed student's *t* test for unpaired data and we observed that the presence of PTEN reduced in a statistically significant ($P<0.001$) manner the efficacy of P529. Effects of PTEN siRNA (D) on IC_{50} values for P529 and comparison of those observed after treatment with equimolar concentration of scramble siRNA. Treatment with siRNA or scramble RNA was performed using the experimental conditions suggested from the producers and was performed 24 h before the treatment with P529. These experiments are representative of three individual experiments. White columns represent data obtained from the analyses assessed at 24 h of treatment, whereas black columns represent data assessed after 48 h of treatment. We performed student's *t* test for unpaired data and we observed that treatment with PTEN siRNA increased significantly ($P<0.001$) the efficacy of P529 in PTEN-positive DU145 cell line.

representation of the effects of 1.0 μM (which is able to reduce about 100% of Akt activity) P529 on TORC1/2 pathways observed in PC3 cell cultures is shown. P529 was able to inhibit TORC1/2 activity at a relatively low concentration as evidenced by the dephosphorylation of $S6^{Ser235/236}$, 4E-$BP^{Thr37/66}$, Akt^{Ser473}, GSK3β^{Ser9}, Fox01a^{Ser256}, $MDM2^{Ser166}$, and $p70S6k^{Thr389}$. The levels of p-Akt (T308) and p-PDK1 (S241) were not modified, suggesting that P529 does not inhibit the phosphorylation of Akt-Thr308 and hence does not affect PDK1.

To assess the activity of P529 on tumor cell proliferation, PCa cell lines were exposed *in vitro* to increasing concentrations of the drug for different times and then analyzed by direct cell count of viable cells and MTS assay. Data were plotted as percent

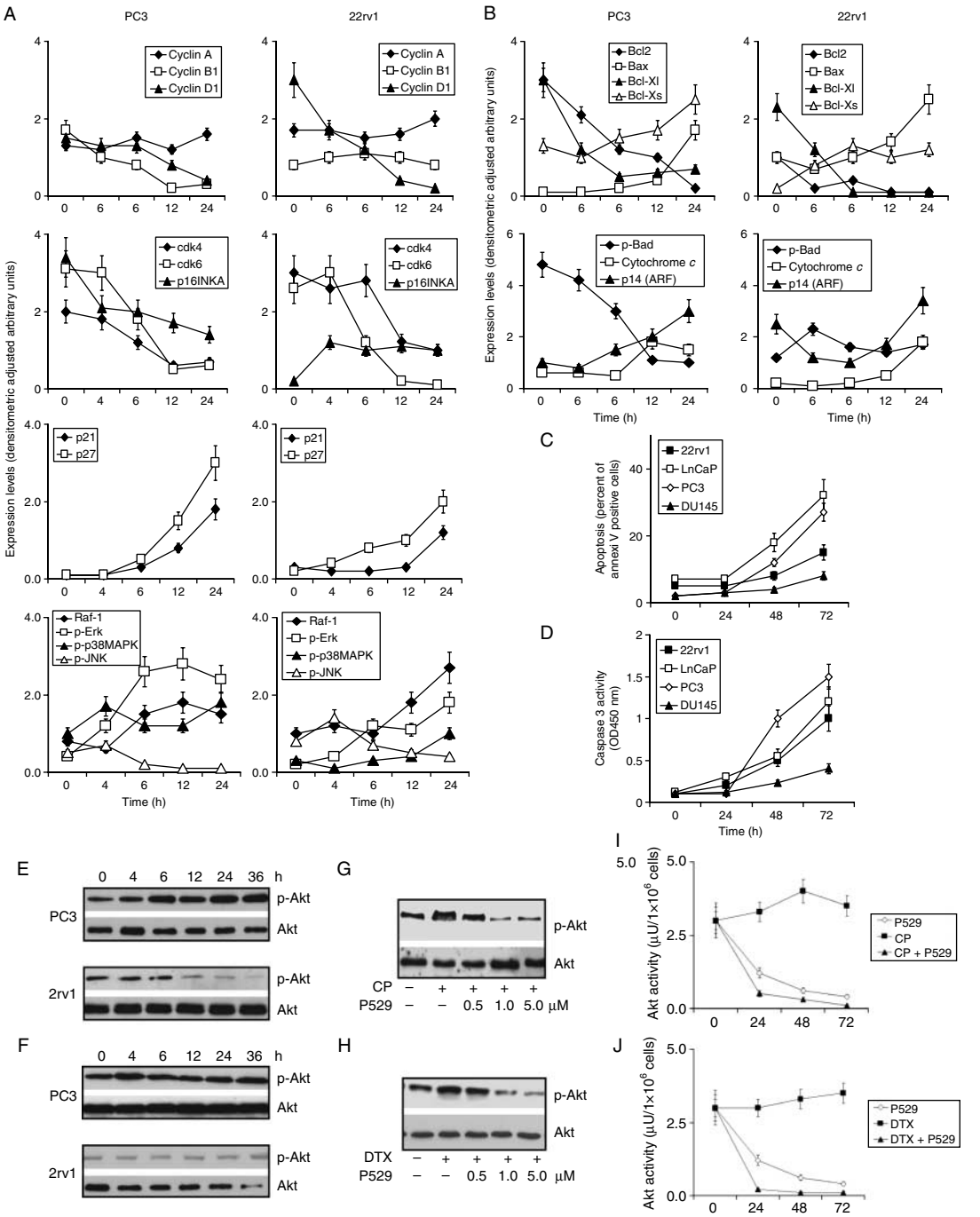

versus controls measured at different times (24, 48, and 72 h) and IC_{50} values were calculated by GrafIt. P529 inhibited the cell proliferation of neoplastic cells at different extent (IC_{50} values ranged from 5 to 28 μM), whereas very few effects were observed in non-neoplastic BPH1 and EPN cells. In Fig. 1B, the representation of P529 effects observed on BPH1 (representative cell line for non-neoplastic prostatic cell line) and on six representative cell lines used as model of 19 cell lines used in this study: i) LnCaP (model of androgen dependent, AR^+, $PTEN^-$ cell line), ii) C4-2B (derivative of LnCaP cell line but with androgen-independent phenotype), iii) LAPC-4 (model of androgen-dependent AR^+, $PTEN^+$ cell line), iv) 22rv1 (model of androgen-independent AR^+, $PTEN^+$ cell line), v) PC3 (model of androgen-independent AR^-, $PTEN^-$ cell line), vi) DU145 (model of androgen-independent AR^-, $PTEN^+$ cell line) is shown. The comparison of IC_{50} values calculated both in PTEN-positive (CWR22 and CWR22R cell derivatives, 22rv1, LAPC-4, VCaP, DuCaP, and Du145) and in PTEN-negative (PC3 and LnCaP with its cell derivatives) cell lines as well as those observed after PTEN transfection of PTEN-negative PC3 cells (Fig. 1C) or PTEN silencing in DU145 cells (Fig. 1D) revealed that absence of PTEN was indicative for a better activity of P529.

The effect of this drug on the expression of proteins involved in the regulation of cell cycle was also evaluated. For these purpose, we used PC3 and 22rv1 cells as high- (PC3) and low-sensitive (22rv1) *in vitro* cell models. The molecular analyses were performed by western blot using P529 concentrations corresponding to the relative IC_{20} values for proliferation parameter (1.0 and 10.0 μM respectively for PC3 and 22rv1) and different times of cultures. P529 markedly reduced the levels of cyclin D1 and B1 as well as of cdk4 and cdk6 (Fig. 2A) and these effects were higher in PC3 when compared with those observed in 22rv1 cell line. These changes were accompanied by increased expression of p21 and p27. In addition, we demonstrated an activation of Erk and p38 MAPK activities with reduced p-JNK activity and modulation of proteins involved in the machinery of apoptosis. Also in this case, the extent of pro-apoptotic protein modulation was higher in PC3 when compared with those observed in 22rv1 cell line. P529 increased in a time-dependent manner the levels of Bcl-Xs and Bax and reduced the Bcl2 and Bcl-Xl expression mainly in PC3 cell line. The phosphorylation status of Bad was reduced by P529, whereas cytochrome *c* and p14 alternate reading frame (ARF) were increased. Next, we analyzed the percentage of cells that undergo apoptosis (Fig. 2C) and caspase 3 activity (Fig. 2D) in

Figure 2 (A and B) Western blot analysis performed on cell extracts harvested from PC3 (cell model of PTEN negative and high P529 responsive) and 22rv1 (cell model of PTEN positive and low P529 responsive) cell lines; single bands were quantified densitometrically and normalized versus actin. The values were expressed as adjusted arbitrary densitometric units (ADU). Time-dependent experiments on the expression and phosphorylation status of cell cycle (cyclins and CdKs), MAPK pathway (Raf-1, Erk, and p38), and apoptosis (Bcl2, Bax, BclXl, BclXs, Bad, cytochrome *c*, and p14 alternate reading frame (ARF) proteins in cells treated with 1.0 (PC3) or 10.0 (22rv1) μM of drug. ANOVA test has been performed to determine the statistical significance of the molecular variations induced by P529. In the panel A, we calculated a $P<0.005$ for the variations of cyclin B1 and D1, cdk4, cdk6 and 16INKA, p21 and p27, raf-1, p-erk, p-p38MAPK, p-Jnk for PC3 cells, whereas the levels of cyclin A were not statistically modified. For 22rv1 cells, the differences were statistically significant for the levels of cyclin D1, cdk4, cdk6, p16INKA, p21, p27, raf-1, p-erk, and p-p38MAPK, whereas the levels of cyclin A, cyclin B1, and p-JNK were not statistically modified. In the panel B, we calculated a $P<0.005$ for the all variations of pro- and anti-apoptotic protein modifications for PC3 cells. For 22rv1 cells, the differences were statistically significant for all proteins analyzed except for the levels of Bad. All together, these data suggest that the effects of P529 was higher in PC3 compared with 22rv1 cells in agreement with further analyses. (C) Percentage of cells that undergo apoptotic events evaluated by Annexin V-positive cells by FACS analyses in four PCa cell lines: PC3 and LnCaP (highly sensitive to P529) and 22rv1 and DU145 (less sensitive to P529) cell lines. Highly P529-sensitive cells were treated with 1.0 μM P529, whereas low P529-sensitive cells were treated with 10.0 μM of drug. Statistical analysis was performed using ANOVA test for linear trend followed by Tukey's test. P529 induced a significant increment ($P<0.001$) of apoptotic cell percentage in PC3, LnCaP, 22rv1, and DU145 PCa cell lines. (D) Caspase 3 activity performed in four PCa cell lines: PC3 and LnCaP (highly sensitive to P529) and 22rv1 and DU145 (less sensitive to P529) cell lines. Highly P529-sensitive cells were treated with 1.0 μM P529, whereas low P529-sensitive cells were treated with 10.0 μM of drug. Statistical analysis was performed using ANOVA test for linear trend followed by Tukey's test. P529 induced a significant increment ($P<0.001$) of caspase 3 activity in PC3, LnCaP, 22rv1, and DU145 PCa cell lines. (E–H) Western blot analysis performed on cell extracts harvested from PC3 (cell model of PTEN negative and high P529 responsive) and 22rv1 (cell model of PTEN positive and low P529 responsive) cell lines. (E) Time-dependent experiments showing the expression and the phosphorylation (ser 473) status of Akt in PC3 and 22rv1 cell lines treated with 10 μg/ml CP. (F) Time-dependent experiments showing the expression and the phosphorylation (ser 473) status of Akt in PC3 and 22rv1 cell lines treated with 10 nM DTX. (G) Dose-dependent reduction of p-Akt after induction of PC3 cell line by 10 μg/ml CP. (H) Dose-dependent reduction of p-Akt after induction of PC3 cell line by 10 nM DTX. Each western blot lane was loaded with 40 μg proteins and normalized versus actin. (I and J) Time-dependent experiments for the enzymatic activity determination of Akt in (I) PC3 cells treated with 10 μg/ml CP and/or 1.0 μM P529 and (J) in PC3 cells treated with 10 nM DTX and/or 1.0 μM P529. Statistical analysis was performed using ANOVA test for linear trend followed by Tukey's test. P529 induced a significant decrement ($P<0.001$) in Akt activity in the time. These data are representative of three individual experiments.

the same cells as well as in other two cell models, LnCaP (highly sensitive to P529) and DU145 (less sensitive to P529) cell lines using the drug concentrations of 1.0 μM (PC3 and LnCaP cell lines) and 10 μM (22rv1 and DU145 cell lines). P529 increased apoptosis ratio and caspase 3 activity in a time-dependent manner and the effects were higher in PC3 and LnCaP compared with DU145 and 22rv1 cell lines.

In vitro effect of P529 in combination with DTX or cispaltin

It has been previously demonstrated that Akt pathways is involved in the response to chemotherapeutic drugs through the induction of Akt activity. Figure 2E and F shows the time-dependent effects of cisplatin (1.0 μg/ml CP, panel E) and DTX (10 nM DTX, panel F) on Akt activity measured in cells treated with 1.0 and 10 μM P529. Pharmacological treatment with P529 reduced Akt activity in CP- and DTX-treated cells in a dose-dependent manner (Fig. 2G and H) at 24 h of treatment with P529 performed after 48 h of treatment with the chemotherapeutical agent. P529 (1.0 μM) was also able to bring down the level of Akt activity to zero at 72 h of treatment (Fig. 2I and J) in PC3 cell model with respect to other treatments ($P<0.001$).

In vitro synergistic anti-tumor effects of P529 in combination with chemotherapeutic agents (cisplatin and DTX)

We used P529 equipotent doses of P529 and CP or DTX administered with different modalities of treatment. We performed different combination treatments, including a sequential schedule with P529 (2 days) followed by DTX or CP (2 days), a second therapeutic approach with DTX or CP (2 days) followed by P529 (2 days) or a simultaneous combination DTX or CP plus P529 for 2 days. We verified the efficacy of these combination treatments in PC3 and 22rv1cell models. Our results demonstrated that P529 was additive/synergistic with DTX and CP (Supplementary Table 1, see section on supplementary data given at the end of this article). The strongest synergism was, however, achieved when PCa cells were sequentially exposed to CP or DTX followed by treatment with P529. Pre-treatment with P529 before the exposure to chemotherapeutic drugs resulted in a moderate synergism, closer to an additive effect expected for the combination with higher concentration of drug. Intermediate values of CI were found when drugs were administered simultaneously. In all combinations, we measured a dose reduction in the IC_{50} values (DRI50) from 1.6- to 4.8-fold for DTX (1.6 to 2.8 in PC3 and 2.4 to 4.8 in 22rv1 cell lines) and from 1.3 to 4.7 for CP (1.4 to 4.7 in PC3 and 1.3 to 2.9 in 22rv1 cells) in combination with P529 compared with the concentrations of the two drugs alone. Further analysis of these data suggests that the combination P529 and DTX shows higher efficacy in 22rv1 cell line, whereas the combination P529 and CP shows higher efficacy in PC3 cells. These differential effects could be due to different effects of CP or DTX in the levels of Akt phosphorylation, as shown in Fig. 2 panels E and F.

Combination of P529 with chemotherapeutic drugs demonstrated a significant reduction of tumor cell viability as evidenced by a dose-dependent chemotherapeutic agent induction of 50% cell death. In particular, the concentration of chemotherapeutic agent able to induce 50% of cell death was reduced significantly. As PC3 cells are exposed simultaneously to 1.0 μM P529 and escalating doses of DTX, a significant reduction of cell viability (Fig. 3A) with acquisition of aberrant phenotypic appearance (Fig. 3B) was observed, as shown in Fig. 3. Measurement of apoptosis revealed an increasing percentage of apoptotic cells (Fig. 3C and D) in combination treatments compared with those observed in single treatments. Analysis of the activity of caspase 3 in drug combination treatments of PC3 and 22rv1 cell models is also shown (Fig. 3E and F). Again, analysis suggests a preferred administration schedule for P529 and cisplatin being the sequence where cisplatin is given prior to P529 administration, whereas for the combination between DTX and P529, greater activity was observed when P529 was added prior to chemotherapeutic drugs (DTX).

In vivo experiments

Effects of P529 as monotherapeutic agent

P529 was able to reduce tumor growth in a dose-dependent manner both in PC3 and 22rv1 xenografts (Fig. 4A and Supplementary Table 2, see section on supplementary data given at the end of this article) confirming the *in vitro* data. A 10, 47.6, and 59.3% reduction of tumor mass was demonstrated in mice bearing PC3 xenografts receiving 50, 100, and 200 mg/kg P529 respectively and a 9, 38.7, and 51.5% reduction of tumor mass in mice bearing 22rv1 xenografts receiving 50, 100, and 200 mg/kg P529 respectively. The proliferation index was also reduced of 4, 34, and 72% in mice bearing PC3 xenografts receiving 50, 100, and 200 mg/kg P529 respectively and of 27, 56, and 60% in mice bearing 22rv1 xenografts receiving 50, 100, and 200 mg/kg P529

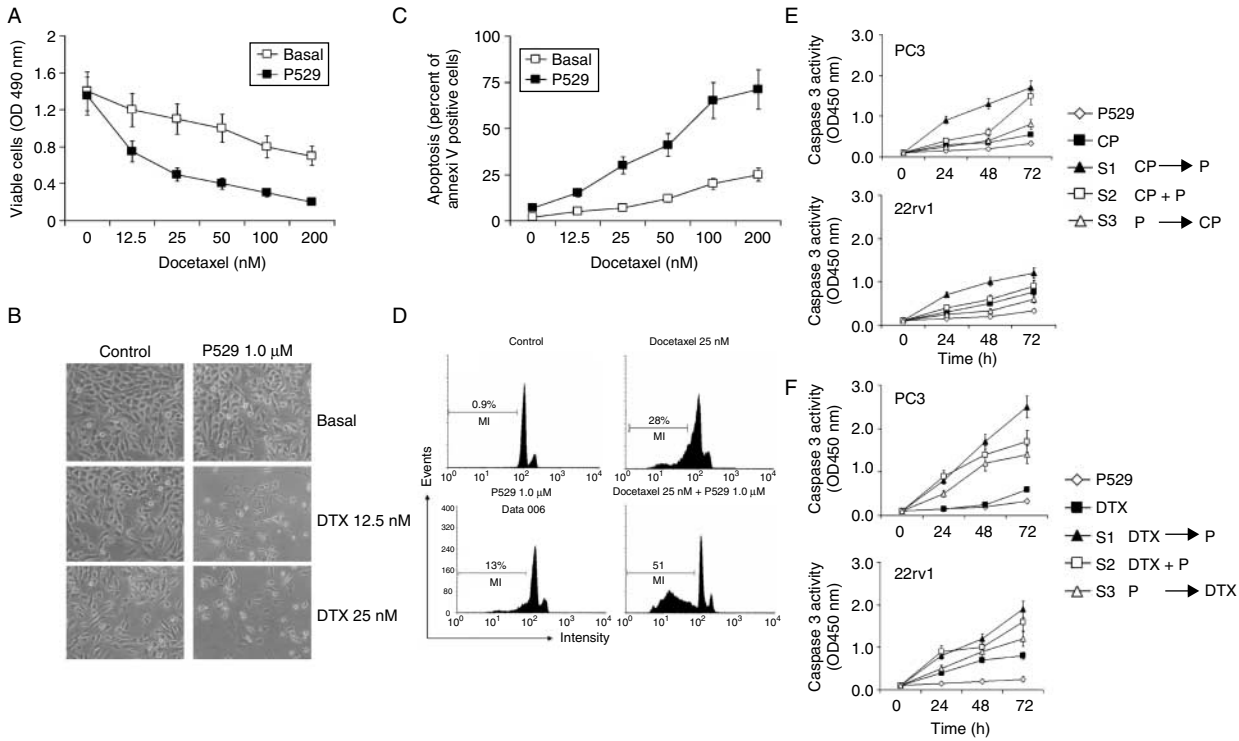

Figure 3 PC3 cells were co-treated for 72 h with P529 (1.0 μM) and different doses of DTX. (A) Viable cells were evaluated using MTT assay and optical density measured at 490 nm. Statistical analysis was performed using ANOVA test for linear trend followed by Tukey's test. DTX induced a significant reduction ($P<0.001$) of viable cell percentage in the PC3 cell line. P529 significantly ($P<0.001$) increased the effects of DTX in the same cells. Comparison between the effects of the DTX alone or in combination with P529 was performed using the Student's *t* test at each DTX concentration and revealed that P529 significantly increased ($P<0.001$) the effects of DTX in the same cells. (B) Morphological appearance at 200× magnification of treated cells. (C) Percentage of PC3 apoptotic cells at different doses of docetaxel in the presence of nontoxic dose (1.0 μM) of P529. (D) Representative FACS determination in PC3 cells treated with P529 (1.0 μM) and DTX (25 nM). Comparison of the effects of combination treatment modalities using 10 μg/ml CP (E) and 10 nM DTX (F) plus 1.0 μM P529 in PC3 and 22rv1 cell lines on apoptosis evaluated through the determination of caspase 3 activity. CP and DTX were administered before (combination S1), simultaneously (S2), or after (S3) P529 administration. This figure shows that the better administration schedules are S1 and S3. Statistical analysis was performed using ANOVA test for linear trend followed by Tukey's test. Comparison between the different treatment modalities was performed using the Student's *t* test at each time of treatment. Our analysis suggests a preferred administration schedule for P529 and cisplatin being the sequence where cisplatin is given prior to P529 administration, whereas for the combination between docetaxel and P529, greater activity was observed when P529 was administered prior to chemotherapeutic drugs (docetaxel).

respectively. Apoptosis was evident in about 8 and 15% of cells in mice bearing PC3 xenografts receiving 100 and 200 mg/kg P529 respectively and in about 8 and 15% of cells in mice bearing PC3 xenografts. In about 5 and 8% of cells in mice bearing 22rv1 xenografts receiving 100 and 200 mg/kg P529, respectively, P529 decreased, in a dose-dependent manner, $CD31^+$ micro-vessels by 24, 41, and 56% in PC-3 receiving mice treated with 50, 100, and 200 mg/kg P529 and by 15, 47, and 73% in 22rv1 receiving mice treated with 50, 100, and 200 mg/kg P529. In Fig. 4B, the microscopic effects of P529 in PC3 tumors are illustrated. In the left columns, Masson Trichrome staining shows large and numerous vessels (stained orange/red fibrin aggregates) in untreated sections. However, with P529 treatment, a marked reduction in the number, size, and stability of the blood vessel bed was observed. At 200 mg/kg P529 treatment, vessels seem to be disrupted with abundant red cells dispersed in the tissue. CD31-positive cells were significantly reduced as shown in the middle panels. VEGF-positive tumor cells were also strongly reduced, indicating a double effect of P529 in angiogenetic neo-vascularization – the first on endothelial cell viability and the second on growth factor support of endothelial cell proliferation.

In vivo synergistic anti-tumor effect of P529 in combination with cisplatin (CP) and DTX

To determine *in vivo* the presence of the synergistic anti-tumor effects that were demonstrated *in vitro*, we evaluated P529 in combination with CP and DTX in

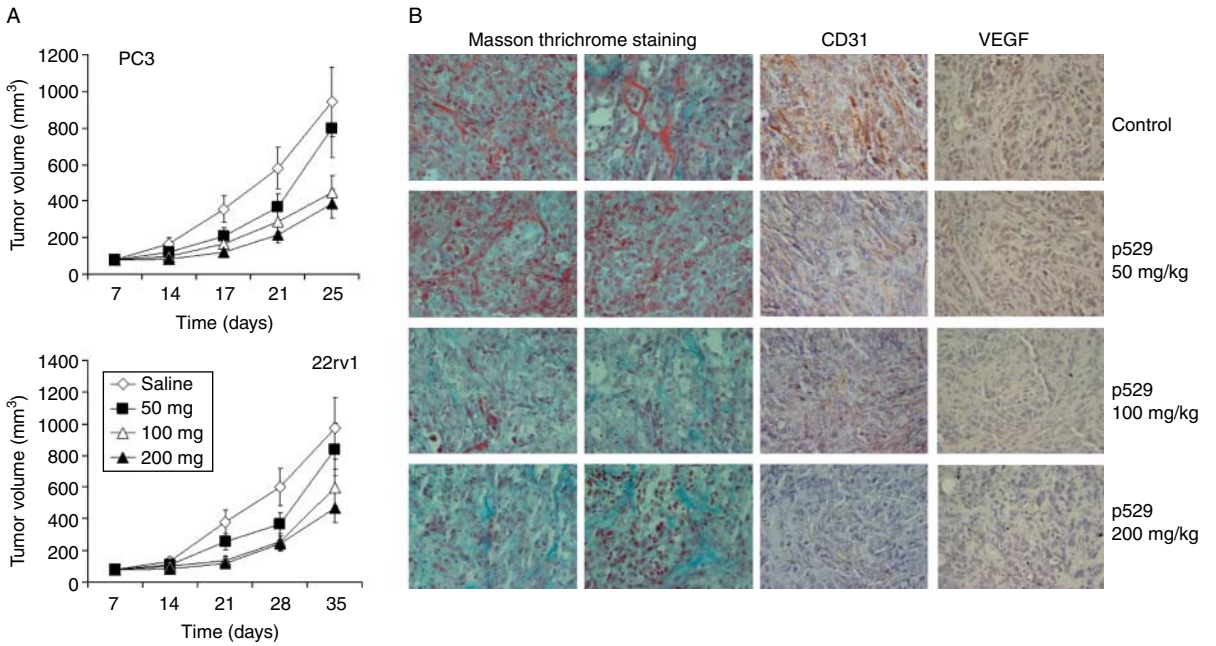

Figure 4 *In vivo* dose-dependent experiments using PC3- and 22rv1-bearing male nude mice treated with 50, 100, and 200 mg/kg P529 administered by oral gavage 7 days after s.c. injection or when tumors arise about 80 mm^3 of size. Tumor volumes were measured weekly. PC3 xenografts arise critical volumes 20–25 days after cell inoculation, whereas these values were raised to 30–35 after 22rv1 cell injection. Experiments were performed using 10 animal for a group and were stopped at indicated times. Statistical analysis was performed using ANOVA test for linear trend followed by Tukey's test. P529 induced a significant dose-dependent reduction ($P<0.001$) of tumor volume in the PC3 and 22rv1 xenografts. Microscopic appearance of PC3 tumors derived from mice treated or not with different doses of P529 (200× magnification). Masson Trichorme staining reveals fibrin (orange/red stain) deposit in enlarged vessels in controls tumors. Administration of P529 reduced fibrin deposit with increased deposition of collagen (Azur stain), increased necrotic zones with cells having picnotic nuclei and blood blending associated with accumulation of granulocytes. The CD31 immunostaining revealed a large amount of vessel in controls and in tumors treated with low dose of P529 (50 mg/kg per day). In the presence of 100 and 200 mg/kg P529, the numbers of CD31-positive endothelial cells, isolated or associated in evident vessels, were reduced as that with VEGF immunostaining supporting a role of PI3K/Akt activation in increased angiogenetic events in cancer.

PC3 and 22rv1 cell xenograft experimental models in athymic nude mice by measuring tumor volume, TGD, CI, and TTP. A total of 144 xenografted mice inoculated with PC3 (72 animals) and 22rv1 (72 animals) were randomly assigned to receive therapeutic doses of P529 (100 mg/kg pos.), CP (5 mg/kg pos.), DTX (20 mg/kg i.p.), and combinations as described in Materials and methods. At day 25, which represents the median survival duration of mice in the control group, the combination treatments induced a significant inhibition in PC3 and 22rv1 tumors (Fig. 5A–D; Tables 1 and 2).

The calculation of combination indices revealed that the combination involving DTX and P529 resulted to be synergistic both in PC3 (CI = 0.34) and 22rv1 (CI = 0.50) xenografts. The combination involving CP and P529 resulted in synergy for the 22rv1 (CI = 0.69) xenograft and additive for the PC3 (CI = 1.13) xenograft. Combined therapy significantly prolonged the TTP defined as the time necessary to have at least an increase of >50% of tumor volume (Fig. 5E and G for PC3 tumors and Fig. 5F and H for 22rv1 tumors). Furthermore, synergistic/additive effects between P529 and CP or DTX were also confirmed by the evaluation of CI reported versus LCK (see Materials and methods). As a consequence, in mice treated with CP, P529, or combined therapy, the number of tumors which are in progression (defined as the increment of tumor volume higher of 50%) was 12/12 (100%), 12/12 (100%), and 7/12 (58.3%) respectively in PC3 tumors (Fig. 5E and G), and 12/12 (100%), 0/12 (100%), and 8/12 (67%) respectively in 22rv1 tumors. In mice treated with DTX, P529, or with combined therapy, the number of tumors which are in progression was 12/12 (100%), 12/12 (100%), and 6/12 (50.0%) respectively in PC3 tumors (Fig. 5E and G), and 12/12 (100%), 12/12 (100%), and 2/12 (16.7%) respectively with 22rv1 tumors (Fig. 5F and H). Stable disease (4/12 (33%) was documented only after combined therapy in 22rv1 xenografts.

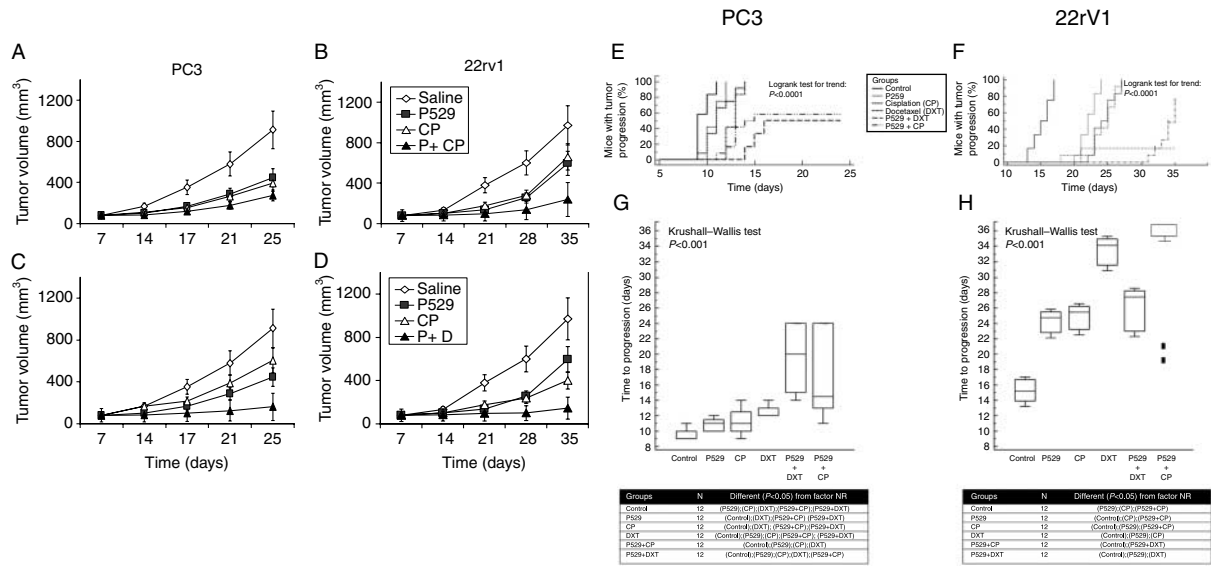

Figure 5 (A and C) Tumor proliferation in PC3 (A) and 22rv1 (C) xenografts in the presence of CP alone or in combination with 100 mg/kg per day P529. Group 1: 10 mice received a 0.2% tyloxapol in Alcon balanced salt solution (vehicle) by oral gavage. Group 2: 10 mice received 100 mg/kg P529 in vehicle by oral gavage/5 day per week. Group 3: 10 mice received i.p. injections of 30.0 mg/kg CP 1 q28 days. Group 4: 10 mice received i.p. injections of 30.0 mg/kg CP (1/q21) followed by 100 mg/kg per 5 days per weeks by oral gavage. Statistical analysis was performed using ANOVA test for linear trend followed by Tukey's test. P529 increased significantly the effects of DTX and CP in the PC3 xenografts. (B and D) Tumor proliferation in PC3(B) and 22rv1 (D) xenografts in the presence of DTX alone or in combination with 100 mg/kg per day P529. Group 1: 10 mice received a 0.2% tyloxapol in Alcon balanced salt solution (vehicle) by oral gavage. Group 2: 10 mice received 100 mg/kg P529 in vehicle by oral gavage/5 day per week. Group 3: 10 mice received i.p. injections of DTX (7.5 mg/kg per week) every week. Group 4: 10 mice received i.p. injections of DTX (7.5 mg/kg per week) every week followed by 100 mg/kg per 5 days per weeks by oral gavage. Statistical analysis was performed using ANOVA test for linear trend followed by Tukey's test. P529 increased significantly the effects of DTX and CP in the 22rv1 xenografts. Proliferation was measured considering the variation of tumor volume (mm^3) in the time (days). Animals were killed at the indicated times of treatment. (E and F) Kaplan–Meyer analysis performed on time to progression parameter on the above-mentioned administration schedule. (G and H) Multi-comparison graph showing the Krushal–Wallis test for the above-mentioned administration schedule.

Discussion and conclusions

One of the major obstacles in curing locally advanced and metastatic PCa is the development of resistance to therapy. Historically, chemotherapy has had limited utility in treating castration-resistant locally advanced and metastatic PCa. Nevertheless, DTX is the standard first-line chemotherapy for this disease (Patel *et al*. 2005, Armstrong *et al*. 2007, Nakabayashi *et al*. 2008, Ross *et al*. 2008, Galsky & Vogelzang 2010). The response to DTX is, however, partial and associated with increased resistance to apoptosis, thus indicating a clear need for new therapies in HRPC patients. Recent report shows that single-agent satraplatin or carboplatin improves PFS as second-line chemotherapy for patients with HRPC (Nakabayashi *et al*. 2008, Ross *et al*. 2008, Reuter *et al*. 2010). Repopulation during courses of chemotherapy is an important cause of drug resistance in patients. The resistance of tumor cells to anti-cancer agents remains a major cause of failure in the treatment of patients with cancer.

Our hypothesis is that short-acting agents that selectively inhibit the proliferation of tumor cells are likely to improve the effectiveness of chemotherapy. In the present study, we use P529 alone or in association with cisplatin or DTX in PCa cells.

P529 has been shown to dissociate both the TORC1 and TORC2 complexes (ref. 1–3). Dissociation of the complexes inhibits both TORC1 and TORC2 signaling, as shown by inhibition of the phosphorylation of S6 via TORC1, phosphorylation of Akt-Ser473 via TORC2, and phosphorylation of GSK3β via TORC2 (1–3). As P529 does not affect PDK1, the phosphorylation of Akt-Thr308 is not inhibited by P529 (1–3). As P529 does not inhibit the phosphorylation of Akt-Thr308, and hence does not affect PDK1, there is no reason to assess either PDK1 or Akt-Thr308 phosphorylation. However, the binding partner of P529 is not known. Hence, although it is possible, it cannot be said that P529 directly interacts with the TORC complexes causing their dissociation. It is also possible

Table 1 Anti-tumor activity of P529 in PC-3 tumors in combination with docetaxel (DTX) or cisplatin (CP). Proliferation index (PI) was measured considering the mean of Ki67 positive cell percentage ± S.D. measured on five random fields at 100×. Apoptosis was measured as the percentage of tunnel-positive cells ± S.D. measured on five random fields (400×). Vessels were measured as the vessel number per field at 100×

Drug	Dose (mg/kg)	Tumors	Weight of mice (g ± S.D.)	Tumor weight (mg ± S.D.)	PI (Ki67%)	Apoptosis	Vessels	Tumor-free mice
Treatment								
Saline		12	25.0 ± 2.0	912 ± 370	37.3 ± 4.5	<2	22.0 ± 4.3	0/12
P529	100	12	24.1 ± 2.1	462 ± 272	11.5 ± 1.5	8.4 ± 2.6	16.4 ± 1.9	0/12
DTX	20	12	23.4 ± 1.9	605 ± 97	31.0 ± 3.3	7.2 ± 2.7	17.5 ± 4.5	0/12
P529 + DTX		12	22.4 ± 2.2	162 ± 181	1.3 ± 1.7	28.2 ± 3.2	12.5 ± 2.5	6/12
CP	5	12	23.7 ± 1.8	392 ± 159	18.5 ± 3.1	18.2 ± 3.2	15.5 ± 3.5	0/12
P529 + CP		12	21.6 ± 3.0	274 ± 222	6.9 ± 0.6	24.3 ± 2.1	11.4 ± 4.4	5/12
Statistics			***P***	***P***	***P***	***P***	***P***	***P***
Saline versus P529			0.294 NS	0.003	<0.001	<0.001	<0.001	NS
Saline versus DTX			0.057 NS	0.011	0.036	<0.001	0.078 NS	NS
Saline versus CP			0.108 NS	<0.001	<0.001	<0.001	<0.001	NS
Saline versus P529 + DTX			0.006	<0.001	<0.001	<0.001	<0.001	0.018
Saline versus P529 + CP			0.004	<0.001	<0.001	<0.001	<0.001	0.044
P529 versus P529 + DTX			0.066 NS	0.004	<0.001	<0.001	<0.001	0.018
P529 versus p529 + CP			0.027	0.077 NS	<0.001	<0.001	<0.001	0.044
DTX versus P529 + DTX			0.246 NS	<0.001	<0.001	<0.001	0.086 NS	0.018
CP versus P529 + CP			0.049	0.149 NS	<0.001	0.007	<0.001	0.044

that P529 may inhibit a chaperone, which assembles the TORC complexes.

To assess the influence of P529 on the cancer growth potential, several PCa (see Materials and methods) and two normal prostate cell lines were treated with different concentrations of drug. P529 was able to effectively inhibit TORC1/2 activity, as evidenced by the dephosphorylation of $S6^{Ser235/236}$, $4E\text{-}BP^{Thr37/66}$, Akt^{Ser473}, $GSK3\beta^{Ser9}$, $Fox01a^{Ser256}$, $MDM2^{Ser166}$, and $p70S6k^{Thr389}$ without any interference with PDK1 activity. The expression levels of p-PDK1 (S241) and p-Akt (T308) were not, indeed, modified by P529 treatment. In addition, treatment with P529 resulted in a concentration-dependent reduction in viable/proliferating tumor cells compared with non-neoplastic BPH1 and EPN cells. IC_{50} values ranged from 5 to 28 μM. P529 showed less effective in PTEN-positive cells compared with PTEN-negative cells, and was similarly observed in transfected PC3 cells, having significant decreased Akt activity, compared with the effects evaluated in parental cells as well as the treatment with PTEN siRNA in DU145 cells with increased levels of Akt activity.

P529 markedly reduced the levels of cyclin D1 and B1 as well as cdk4 and cdk6. These changes were accompanied by increased expression of p21 and p27 and an accumulation of cells in G0/G1 followed to apoptosis associated with mitochondrial damage and activation of caspase 3.

Apoptosis was associated with the induction of pErk and p-p38MAPK and loss of p-JNK. This may seem paradoxical, as JNK is a key mediator of apoptosis in prostate cells. We rather believe that this is not the case since several reports indicate a differential involvement of ERK, p38 MAPK, and JNK in apoptosis and/or proliferation (Dondi *et al*. 2006, Hao *et al*. 2007, Li *et al*. 2007, Cao *et al*. 2010, Festuccia *et al*. 2010, Reddivari *et al*. 2010, Xiao *et al*. 2011). We presume that it is rather the ratios between the activities of p38MAPK and JNK, Erk, and p38MAPK and Erk and JNK that may diversify tumor cell destiny after a pharmacologic treatment.

P529 was examined for modulation of Akt activity induced after treatment with low doses (non-toxic) of cisplatin and DTX. P529 was also evaluated in combination administration with DTX and CP. With *in vitro* testing, P529 showed additive/synergistic with DTX and CP, with the strongest synergism achieved when PCa cells were sequentially exposed to CP or DTX followed by treatment with P529 or when drugs were administered simultaneously. Treatment with P529 before exposure to chemotherapeutic drugs resulted in a moderate synergism, closer to an additive effect. The effects of combined treatment with cisplatin

Table 2 Anti-tumor activity of P529 in 22rv1 tumors in combination with docetaxel (DTX) or cisplatin (CP). Proliferation index (PI) was measured considering the mean of Ki67-positive cell percentage ± S.D. measured on five random fields at 100×. Apoptosis was measured as the percentage of tunnel-positive cells ± S.D. measured on five random fields (400×). Vessels were measured as the vessel number per field at 100×

Drug	Dose (mg/kg)	Tumors	Weight of mice (g ± S.D.)	Tumor weight (mg ± S.D.)	PI (Ki67%)	Apoptosis	Vessels	Tumor-free mice
Treatment								
Saline		12	25.5 ± 2.2	1058 ± 250	28.6 ± 4.5	<2	36.5 ± 3.5	0/12
P529	100	12	24.0 ± 1.7	657 ± 149	15.4 ± 5.1	10.2 ± 1.5	27.5 ± 3.0	0/12
DTX	20	12	22.9 ± 2.0	402 ± 111	12.5 ± 2.2	15.1 ± 2.0	15.6 ± 1.3	0/12
P529 + DTX		12	21.8 ± 2.6	126 ± 49	8.3 ± 1.4	34.3 ± 2.5	7.5 ± 1.0	5/12
CP	5	12	23.6 ± 1.5	860 ± 116	25.3 ± 3.9	<2	31.5 ± 4.5	0/12
P529 + CP		12	20.8 ± 2.8	240 ± 112	7.59 ± 2.0	24.4 ± 8.0	9.4 ± 4.4	3/12
Statistics			***P***	***P***	***P***	***P***	***P***	***P***
Saline versus P529			0.075 NS	<0.001	0.002	<0.001	<0.001	NS
Saline versus DTX			0.006	<0.001	<0.001	<0.001	<0.001	NS
Saline versus CP			0.038	0.021	0.250 NS	NS	<0.001	NS
Saline versus P529 + DTX			0.001	<0.001	<0.001	<0.001	<0.001	0.044
Saline versus P529 + CP			<0.001	<0.001	<0.001	<0.001	<0.001	0.217 NS
P529 versus P529 + DTX			0.023	<0.001	0.017	<0.001	<0.001	0.044
P529 versus p529 + CP			0.003	<0.001	<0.001	<0.001	<0.001	0.217 NS
DTX versus P529 + DTX			0.258 NS	<0.001	0.007	<0.001	0.086 NS	0.044
CP versus P529 + CP			0.003	<0.001	<0.001	<0.001	<0.001	0.217 NS

or DTX followed by a P529 administration resulted in higher *in vitro* effects both in PTEN-negative and in PTEN-positive PCa cells.

These effects were maintained *in vivo* both in PTEN-positive 22rv1 xenografts and PTEN-negative PC3 xenografts cultured in male nude mice. Administration of P529 to nude male mice receiving 22rv1 and PC3 cells xenografts results in a modest and hence insignificant reduction of animal weight. Dose-ranging toxicology studies in both rats and dogs with P529 showed no toxicities at doses above that given to mice in studies described here (toxicology studies carried out by Paloma Pharmaceuticals, personal communication). Significant reduction in weight of treated animals was found only when P529 was associated to DTX and CP and this seemed primarily to be due to the side effects of DTX as indicated to the loss of statistical significance in the comparisons between DTX effects and combinations with P529. Significant statistical difference was observed in the comparison with CP and CP plus P529 administration, suggesting a cumulative effect of two drugs. Nevertheless, the analyses of *in vivo* effects show that the combination of P529 with DTX or CP was synergistic both in PC3 and 22rv1 tumor models with increased percentage of complete and partial responses. Furthermore, the percentage of tumor that was in progression was sensitively reduced and the TTP significantly increased compared with those observed with single treatments. Taken together, our studies indicate that TORC1/2 downmodulation represents a useful therapeutic approach for enhancing chemosensitivity of PCa to DTX and cispaltin and provide a rationale for clinical trials on combination treatments with P529 in patients with advanced prostate tumors.

Translational relevance

HRPC is an advanced chemo-resistant disease wherein treatment options are mostly palliative. The overall effect of chemotherapy on a tumor depends on the amount of tumor cell kill achieved with each course and the extent of repopulation of surviving tumor cells between courses of chemotherapy. There is evidence that the proliferation of surviving tumor cells may increase after chemotherapy and that the rate of repopulation after sequential treatments with chemotherapy may accelerate with time. Activation of PI3K/Akt/mTOR pathways is often observed during PCa progression. Our studies provide pre-clinical evidence that the inhibition of this pathways is a very effective approach to treat HRPC. We targeted Akt/mTOR pathways by using an oral available TORC1/TORC2 inhibitor (P529) and showed that this agent shows synergistic effects with DTX and

cisplatin. These results provide a rationale to a clinical development with conventional chemotherapy and inhibitors of the PI3K/Akt/mTOR pathway.

Supplementary data

This is linked to the online version of the paper at http://dx.doi.org/10.1530/ERC-11-0045.

Declaration of interest

D S is President and CEO of Paloma Pharmaceuticals, Inc. The other authors disclosed no potential conflicts of interest.

Funding

The work is partially supported by Paloma Pharmaceuticals, Inc. (Jamaica Plain, MA, USA).

References

Armstrong AJ, Garrett-Mayer ES, Yang YC, de Wit R, Tannock IF & Eisenberger M 2007 A contemporary prognostic nomogram for men with hormone-refractory metastatic prostate cancer: a TAX327 study analysis. *Clinical Cancer Research* **13** 6396–6403. (doi:10.1158/1078-0432.CCR-07-1036)

Banach-Petrosky W, Jessen WJ, Ouyang X, Gao H, Rao J, Quinn J, Aronow BJ & Abate-Shen C 2007 Prolonged exposure to reduced levels of androgen accelerates prostate cancer progression in Nkx3.1; Pten mutant mice. *Cancer Research* **67** 9089–9096. (doi:10.1158/0008-5472.CAN-07-2887)

Bedolla R, Prihoda TJ, Kreisberg JI, Malik SN, Krishnegowda NK, Troyer DA & Ghosh PM 2007 Determining risk of biochemical recurrence in prostate cancer by immunohistochemical detection of PTEN expression and Akt activation. *Clinical Cancer Research* **13** 3860–3867. (doi:10.1158/1078-0432.CCR-07-0091)

Bertram J, Peacock JW, Fazli L, Mui AL, Chung SW, Cox ME, Monia B, Gleave ME & Ong CJ 2006 Loss of PTEN is associated with progression to androgen independence. *Prostate* **66** 895–902. (doi:10.1002/pros.20411)

Bonaccorsi L, Carloni V, Muratori M, Salvadori A, Giannini A, Carini M, Serio M, Forti G & Baldi E 2000 Androgen receptor expression in prostate carcinoma cells suppresses alpha6beta4 integrin-mediated invasive phenotype. *Endocrinology* **141** 3172–3182. (doi:10.1210/en.141.9.3172)

Bruzzese F, Di Gennaro E, Avallone A, Pepe S, Arra C, Caraglia M, Tagliaferri P & Budillon A 2006 Synergistic antitumor activity of epidermal growth factor receptor tyrosine kinase inhibitor gefitinib and IFN-alpha in head and neck cancer cells *in vitro* and *in vivo*. *Clinical Cancer Research* **12** 617–625. (doi:10.1158/1078-0432.CCR-05-1671)

Calabrò F & Sternberg CN 2007 Current indications for chemotherapy in prostate cancer patients. *European Urology* **51** 17–26. (doi:10.1016/j.eururo.2006.08.013)

Cao H, Feng Q, Xu W, Li X, Kang Z, Ren Y & Du L 2010 Genipin induced apoptosis associated with activation of the c-Jun NH2-terminal kinase and p53 protein in HeLa cells. *Biological & Pharmaceutical Bulletin* **33** 1343–1348. (doi:10.1248/bpb.33.1343)

Chay CH, Cooper CR, Gendernalik JD, Dhanasekaran SM, Chinnaiyan AM, Rubin MA, Schmaier AH & Pienta KJ 2002 A functional thrombin receptor (PAR1) is expressed on bone-derived prostate cancer cell lines. *Urology* **60** 760–765. (doi:10.1016/S0090-4295(02)01969-6)

Chou TC & Talay P 1987 Applications of the median-effect principle for the assessment of low-dose risk of carcinogens for the quantification of synergism and antagonism of chemotherapeutic agents. In *New avenues in developmental cancer chemotherapy*, pp 37–64. Eds KR Harrap & TA Connors. Bristol-Myers Symposium Series. New York, NY, USA: Academic Press.

Craft N, Shostak Y, Carey M & Sawyers CL 1999 A mechanism for hormone-independent prostate cancer through modulation of androgen receptor signaling by the HER-2/neu tyrosine kinase. *Nature Medicine* **5** 280. (doi:10.1038/6495)

Desireddi NV, Roehl KA, Loeb S, Yu X, Griffin CR, Kundu SK, Han M & Catalona WJ 2007 Improved stage and grade-specific progression-free survival rates after radical prostatectomy in the PSA era. *Urology* **70** 950–955. (doi:10.1016/j.urology.2007.06.1119)

Diaz R, Nguewa PA, Diaz-Gonzalez JA, Hamel E, Gonzalez-Moreno O, Catena R, Serrano D, Redrado M, Sherris D & Calvo A 2009 The novel Akt inhibitor Palomid 529 (P529) enhances the effect of radiotherapy in prostate cancer. *British Journal of Cancer* **100** 932–940. (doi:10.1038/sj.bjc.6604938)

Di Gennaro E, Piro G, Chianese MI, Franco R, Di Cintio A, Moccia T, Luciano A, de Ruggiero I, Bruzzese F, Avallone A *et al.* 2010 Vorinostat synergises with capecitabine through upregulation of thymidine phosphorylase. *British Journal of Cancer* **103** 1680–1691. (doi:10.1038/sj.bjc.6605969)

Dondi D, Festuccia C, Piccolella M, Bologna M & Motta M 2006 GnRH agonists and antagonists decrease the metastatic progression of human prostate cancer cell lines by inhibiting the plasminogen activator system. *Oncology Reports* **15** 393–400.

El Sheikh SS, Romanska HM, Abel P, Domin J & Lalani el-N 2008 Predictive value of PTEN and AR coexpression of sustained responsiveness to hormonal therapy in prostate cancer – a pilot study. *Neoplasia* **10** 949–953.

Festuccia C, Gravina GL, Muzi P, Pomante R, Ventura L, Vessella RL, Vicentini C & Bologna M 2007 Bicalutamide increases phospho-Akt levels through Her2 in patients with prostate cancer. *Endocrine-Related Cancer* **14** 601–611. (doi:10.1677/ERC-07-0118)

Festuccia C, Gravina GL, Muzi P, Millimaggi D, Dolo V, Vicentini C & Bologna M 2008 Akt down-modulation

induces apoptosis of human prostate cancer cells and synergizes with EGFR tyrosine kinase inhibitors. *Prostate* **68** 965–974. (doi:10.1002/pros.20757)

Festuccia C, Dondi D, Piccolella M, Locatelli A, Gravina GL, Tombolini V & Motta M 2010 Ozarelix, a fourth generation GnRH antagonist, induces apoptosis in hormone refractory androgen receptor negative prostate cancer cells modulating expression and activity of death receptors. *Prostate* **70** 1340–1349. (doi:10.1002/pros.21169)

Galsky MD & Vogelzang NJ 2010 Docetaxel-based combination therapy for castration-resistant prostate cancer. *Annals of Oncology* **21** 2135–2144. (doi:10.1093/annonc/mdq050)

Graff JR, Konicek BW, McNulty AM, Wang Z, Houck K, Allen S, Paul JD, Hbaiu A, Goode RG, Sandusky GE *et al.* 2000 Increased AKT activity contributes to prostate cancer progression by dramatically accelerating prostate tumor growth and diminishing p27Kip1 expression. *Journal of Biological Chemistry* **275** 24500–24505. (doi:10.1074/jbc.M003145200)

Ha S, Ruoff R, Kahoud N, Franke TF & Logan SK 2011 Androgen receptor levels are upregulated by Akt in prostate cancer. *Endocrine-Related Cancer* **18** 245–255. (doi:10.1530/ERC-10-0204)

Hao F, Tan M, Xu X, Han J, Miller DD, Tigyi G & Cui MZ 2007 Lysophosphatidic acid induces prostate cancer PC3 cell migration via activation of LPA(1), p42 and p38alpha. *Biochimica et Biophysica Acta* **1771** 883–889.

Igawa T, Lin FF, Lee MS, Karan D, Batra SK & Lin MF 2002 Establishment and characterization of androgen-independent human prostate cancer LNCaP cell model. *Prostate* **50** 222. (doi:10.1002/pros.10054)

Kokontis JM, Hay N & Liao S 1998 Progression of LNCaP prostate tumor cells during androgen deprivation: hormone-independent growth, repression of proliferation by androgen, and role for p27Kip1 in androgen-induced cell cycle arrest. *Molecular Endocrinology* **12** 941. (doi:10.1210/me.12.7.941)

Li M, Xiao L & Li Z 2007 The relationship between p38MAPK and apoptosis during paclitaxel resistance of ovarian cancer cells. *Journal of Huazhong University of Science and Technology. Medical Sciences* **27** 725–728. (doi:10.1007/s11596-007-0628-6)

Lin DL, Tarnowski CP, Zhang J, Dai J, Rohn E, Patel AH, Morris MD & Keller ET 2001 Bone metastatic LNCaP-derivative C4-2B prostate cancer cell line mineralizes *in vitro*. *Prostate* **47** 212. (doi:10.1002/pros.1065)

Ma X, Ziel-van der Made AC, Autar B, van der Korput HA, Vermeij M, van Duijn P, Cleutjens KB, de Krijger R, Krimpenfort P, Berns A *et al.* 2005 Targeted biallelic inactivation of Pten in the mouse prostate leads to prostate cancer accompanied by increased epithelial cell proliferation but not by reduced apoptosis. *Cancer Research* **65** 5730–5739. (doi:10.1158/0008-5472.CAN-04-4519)

Murillo H, Huang H, Schmidt LJ, Smith DI & Tindall DJ 2001 Role of PI3K signaling in survival and progression of LNCaP prostate cancer cells to the androgen refractory state. *Endocrinology* **142** 4795–4805. (doi:10.1210/en.142.11.4795)

Nakabayashi M, Sartor O, Jacobus S, Regan MM, McKearn D, Ross RW, Kantoff PW, Taplin ME & Oh WK 2008 Response to docetaxel/carboplatin-based chemotherapy as first- and second-line therapy in patients with metastatic hormone-refractory prostate cancer. *BJU International* **101** 308–312. (doi:10.1111/j.1464-410X.2007.07331.x)

Patel AR, Sandler HM & Pienta KJ 2005 Radiation Therapy Oncology Group 0521: a phase III randomized trial of androgen suppression and radiation therapy versus androgen suppression and radiation therapy followed by chemotherapy with docetaxel/prednisone for localized, high-risk prostate cancer. *Clinical Genitourinary Cancer* **4** 212–214. (doi:10.3816/CGC.2005.n.035)

Pienta KJ, Abate-Shen C, Agus DB, Attar RM, Chung LW, Greenberg NM, Hahn WC, Isaacs JT, Navone NM, Peehl DM *et al.* 2008 The current state of preclinical prostate cancer animal models. *Prostate* **68** 629. (doi:10.1002/pros.20726)

Prewett MC, Hooper AT, Bassi R, Ellis LM, Waksal HW & Hicklin DJ 2002 Enhanced antitumor activity of anti-epidermal growth factor receptor monoclonal antibody IMC-C225 in combination with irinotecan (CPT-11) against human colorectal tumor xenografts. *Clinical Cancer Research* **8** 994–1003.

Reddivari L, Vanamala J, Safe SH & Miller JC Jr 2010 The bioactive compounds alpha-chaconine and gallic acid in potato extracts decrease survival and induce apoptosis in LNCaP and PC3 prostate cancer cells. *Nutrition and Cancer* **62** 601–610. (doi:10.1080/01635580903532358)

Reuter CW, Morgan MA, Ivanyi P, Fenner M, Ganser A & Grünwald V 2010 Carboplatin plus weekly docetaxel as salvage chemotherapy in docetaxel-resistant and castration-resistant prostate cancer. *World Journal of Urology* **28** 391–398. (doi:10.1007/s00345-010-0527-5)

Ross RW, Beer TM, Jacobus S, Bubley GJ, Taplin ME, Ryan CW, Huang J & Oh WK 2008 Prostate Cancer Clinical Trials Consortium. A phase 2 study of carboplatin plus docetaxel in men with metastatic hormone-refractory prostate cancer who are refractory to docetaxel. *Cancer* **112** 521–526. (doi:10.1002/cncr.23195)

Scaccianoce E, Festuccia C, Dondi D, Guerini V, Bologna M, Motta M & Poletti A 2003 Characterization of prostate cancer DU145 cells expressing the recombinant androgen receptor. *Oncology Research* **14** 101–112.

Shukla S, Maclennan GT, Marengo SR, Resnick MI & Gupta S 2005 Constitutive activation of P I3 K-Akt and NF-kappaB during prostate cancer progression in autochthonous transgenic mouse model. *Prostate* **64** 224–239. (doi:10.1002/pros.20217)

Sinisi AA, Chieffi P, Pasquali D, Kisslinger A, Staibano S, Bellastella A & Tramontano D 2002 EPN: a novel

epithelial cell line derived from human prostate tissue. *In Vitro Cellular & Developmental Biology. Animal* **23** 165. (doi:10.1290/1071-2690(2002)038<0165:EANECL>2.0.CO;2)

Sramkoski RM, Pretlow TG II, Giaconia JM, Pretlow TP, Schwartz S, Sy MS, Marengo SR, Rhim JS, Zhang D & Jacobberger JW 1999 A new human prostate carcinoma cell line, 22Rv1. *In Vitro Cellular & Developmental Biology. Animal* **35** 403–409. (doi:10.1007/s11626-999-0115-4)

Svatek RS, Lee JJ, Roehrborn CG, Lippman SM & Lotan Y 2008 Cost-effectiveness of prostate cancer chemoprevention: a quality of life-years analysis. *Cancer* **112** 1058–1065. (doi:10.1002/cncr.23276)

Tepper CG, Boucher DL, Ryan PE, Ma AH, Xia L, Lee LF, Pretlow TG & Kung HJ 2002 Characterization of a novel androgen receptor mutation in a relapsed CWR22 prostate cancer xenograft and cell line. *Cancer Research* **62** 6606–6614.

Trotman LC, Niki M, Dotan ZA, Koutcher JA, Di Cristofano A, Xiao A, Khoo AS, Roy-Burman P, Greenberg NM, Van Dyke T *et al.* 2003 Pten dose dictates cancer progression in the prostate. *PLoS Biology* **1** E59. (doi:10.1371/journal.pbio.0000059)

Uzgare AR & Isaacs JT 2004 Enhanced redundancy in Akt and mitogen-activated protein kinase-induced survival of malignant versus normal prostate epithelial cells. *Cancer Research* **64** 6190–6199. (doi:10.1158/0008-5472.CAN-04-0968)

Verhagen PC, van Duijn PW, Hermans KG, Looijenga LH, van Gurp RJ, Stoop H, van der Kwast TH & Trapman J 2006 The PTEN gene in locally progressive prostate cancer is preferentially inactivated by bi-allelic gene deletion. *Journal of Pathology* **208** 699–707. (doi:10.1002/path.1929)

Wang S, Gao J, Lei Q, Rozengurt N, Pritchard C, Jiao J, Thomas GV, Li G, Roy-Burman P, Nelson PS *et al.* 2003 Prostate-specific deletion of the murine Pten tumor suppressor gene leads to metastatic prostate cancer. *Cancer Cell* **4** 209–221. (doi:10.1016/S1535-6108(03)00215-0)

Wu X, Senechal K, Neshat MS, Whang YE & Sawyers CL 1998 The PTEN/MMAC1 tumor suppressor phosphatase functions as a negative regulator of the phosphoinositide 3-kinase/Akt pathway. *PNAS* **95** 15587. (doi:10.1073/pnas.95.26.15587)

Xiang T, Jia Y, Sherris D, Li S, Wang H, Lu D & Yang Q 2011 Targeting the Akt/mTOR pathway in Brca1-deficient cancers. *Oncogene* **30** 2443–2450. (doi:10.1038/onc.2010.603)

Xiao D, Zeng Y, Prakash L, Badmaev V, Majeed M & Singh SV 2011 ROS-dependent apoptosis by gugulipid extract of ayurvedic medicine plant *Commiphora mukul*, in human prostate cancer cells is regulated by c-JUN N-terminal kinase. *Molecular Pharmacology* **79** 499–507. (doi:10.1124/mol.110.068551)

Xu Y, Chen SY, Ross KN & Balk SP 2006 Androgens induce prostate cancer cell proliferation through mammalian target of rapamycin activation and post-transcriptional increases in cyclin D proteins. *Cancer Research* **66** 7783–7792. (doi:10.1158/0008-5472.CAN-05-4472)

Xue Q, Hopkins B, Perruzzi C, Udayakumar D, Sherris D & Benjamin LE 2008 Palomid 529, a novel small-molecule drug, is a TORC1/TORC2 inhibitor that reduces tumor growth, tumor angiogenesis, and vascular permeability. *Cancer Research* **68** 9551–9557. (doi:10.1158/0008-5472.CAN-08-2058)

Zhao H, Dupont J, Yakar S, Karas M & LeRoith D 2004 PTEN inhibits cell proliferation and induces apoptosis by downregulating cell surface IGF-IR expression in prostate cancer cells. *Oncogene* **23** 786–794. (doi:10.1038/sj.onc.1207162)

Received in final form 18 April 2011
Accepted 28 April 2011
Made available online as an Accepted Preprint
6 May 2011